

## States excited in $^{146}\text{Nd}$ by thermal and average-resonance neutron-capture gamma rays\*

David L. Bushnell

*Physics Department, Northern Illinois University, DeKalb, Illinois 60115  
and Argonne National Laboratory, Argonne, Illinois 60439*

Gianni R. Tassotto

*Physics Department, Northern Illinois University, DeKalb, Illinois 60115*

Robert K. Smither

*Physics Division, Argonne National Laboratory, Argonne, Illinois 60439*

(Received 1 December 1975)

Thermal neutron capture in enriched and natural neodymium targets and average-resonance neutron capture in natural-neodymium targets yield high- and medium-energy  $\gamma$ -ray spectra. These spectra are compared with each other to determine the energies and relative intensities of  $\gamma$  rays from  $^{146}\text{Nd}$  which are then used to construct a partial level scheme for  $^{146}\text{Nd}$ . A cooled intrinsic-germanium detector is used in both coincidence and anticoincidence modes of operation to measure the spectra. Of 146  $\gamma$  rays observed in the 400 to 2800 keV range, 56 are located as transitions among 33 states. Thirty-one primary transitions following average neutron capture are used to describe all but one of the excited states. Most of the states are newly reported here with definite parity assignments and restricted spin choices. A search for the  $2^+$  member of a previously suggested two-phonon triplet indicates that the existence of this member is not likely. The capture state energy is determined to be  $7564.7 \pm 0.4$  keV.

NUCLEAR REACTIONS  $^{145}\text{Nd}(n, \gamma)$ ,  $E_n$ =thermal, measured  $E_\gamma$ ,  $I_\gamma$ , 0.45–2.85 MeV, 4.5–7.1 MeV, intrinsic germanium detector (IGD), thermal neutrons; measured  $E_\gamma$ ,  $I_\gamma$ , 4.5–7.1 MeV, average resonance neutrons IGD; level scheme for  $^{146}\text{Nd}$ ,  $J^\pi$ ,  $\gamma$ -ray branching.

### I. INTRODUCTION

The  $\beta$  decay of  $^{146}\text{Pr}$  to levels in  $^{146}\text{Nd}$  was used by Daniels, Lawrence, and Hoffman<sup>1</sup> to propose a partial level scheme for the  $^{146}\text{Nd}$  nucleus up to 3819 keV.  $\gamma$ - $\gamma$  and  $\gamma$ - $\beta$  coincidence measurements and some  $\gamma$ - $\gamma$  directional correlations based on Ge(Li) detector spectra were employed to suggest a  $^{146}\text{Nd}$  level scheme. They found 12 levels below 2.5 MeV. An earlier similar study using the same 24-min  $\beta$  decay was reported by Ramayya and Yoshizawa<sup>2</sup> who observed seven excited states below 2.5 MeV using scintillation (NaI) spectrometers.  $\beta$ -decay experiments using  $^{146}\text{Pm}$  ( $\sim 1500$  day) to populate states in  $^{146}\text{Nd}$  have been reported by Buss, Funk, and Mihelich<sup>3</sup>; by Taylor and Kukoc<sup>4</sup>; and also by Avotina, Grigor'ev, Zolotov, Sergeev, Sovtsov, Weiss, Urbanec, Vrzal, and Liptak<sup>5</sup> in all three of which the first three excited states were examined. Many of the same states as reported by Daniels *et al.*<sup>1</sup> were observed by Oakey and McFarlane<sup>6</sup> using the  $^{149}\text{Sm}(n, \alpha)^{146}\text{Nd}$  reaction and earlier by Poortmans, Ceulemans, Deruytter, and Neve De Mevergnies.<sup>7</sup> Also elastic and inelastic deuteron scattering and Coulomb excitation with  $\alpha$  particles were used by Christensen, Løvholden, and Rasmussen<sup>8</sup> to describe states in the  $^{146}\text{Nd}$  nucleus. They compared the resulting

level scheme with that of  $^{124}\text{Te}$  which could be expected to have similar vibrational characteristics. Thermal-neutron-capture  $\gamma$ -ray experiments giving information about levels in  $^{146}\text{Nd}$  have been reported by Groshev, Dvoretzskii, Demidov, and Rakhimov<sup>9</sup> and by Berzin, Kruminya, and Prokof'ev.<sup>10</sup> In the latter case, a level scheme was constructed which contains the placement of 25 secondary  $\gamma$ -ray transitions among 19 levels below 2.53 MeV. Several studies which provide additional data on both primary and secondary  $\gamma$  transitions are based on thermal-neutron capture in aligned nuclei as reported by Reddingius, Potters, and Postma<sup>11</sup> and by Reddingius.<sup>12</sup>

The data used in our work are based upon neutron capture in  $^{145}\text{Nd}$  that produces an excited state in  $^{146}\text{Nd}$  at 7564.7 keV which then decays by  $\gamma$  transitions primarily to low-lying levels. For medium- to heavy-weight nuclei the high-energy portion (typically 4.5 to 7.5 MeV) of the resulting  $\gamma$ -ray spectrum is made up entirely of transitions from the capture state and we refer to these as primary transitions. The low-energy end of the  $\gamma$ -ray spectrum (energies less than about 3 MeV) is made up of secondary transitions among the low-energy states. The energy range between the above two ranges is crowded with so many  $\gamma$  rays that it appears as a high background region with

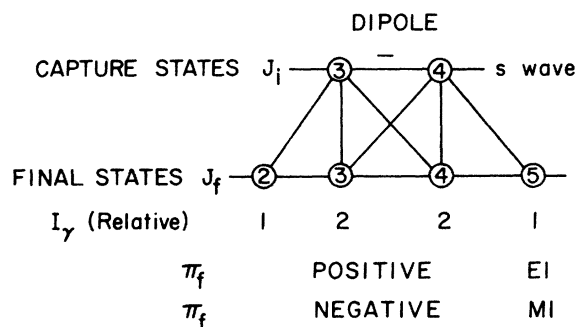


FIG. 1. Possible primary  $\gamma$ -transition routes from the capture state ( $i$ ) to final states ( $f$ ) following  $s$ -wave neutron capture by the  $^{145}\text{Nd}$  nucleus ( $\frac{1}{2}^-$  ground state). Quadrupole transition intensities are either at or below the sensitivity of the present data and therefore the corresponding decay routes are not included here.

relatively little line structure resolved. In addition to thermal-neutron capture, we have used the average-resonance neutron-capture technique developed by Bollinger and Thomas.<sup>13</sup>

The ground state of  $^{145}\text{Nd}$  is known to have negative parity and a spin of  $\frac{7}{2}$ .<sup>14</sup> Therefore, neutrons captured in  $^{145}\text{Nd}$  produce capture states in  $^{146}\text{Nd}$  having  $J^\pi = 3^-$  and  $4^-$ . The final states obtained following  $s$ -wave average capture and dipole primary transitions are shown in Fig. 1. We are not able in the present study to observe quadrupole transitions nor the effect of  $E1$  transitions following  $p$ -wave capture on the line shape of the  $M1$  transitions following  $S$ -wave capture. The information obtained from our experiments is combined with the previous published work to further develop the level scheme of  $^{146}\text{Nd}$ . Twelve pre-

viously suggested states are confirmed and 19 new states are proposed. Parity assignments are confirmed for 9 states and new parity assignments are made for 24 levels. Limits are placed on the spin assignments for 31 levels. Twenty-four of these are new assignments.

## II. EXPERIMENTAL PROCEDURES

### Facilities and targets

The experimental system which was used in this research employs a 4-cm<sup>3</sup> intrinsic-germanium detector located in a Compton-suppression pair spectrometer.<sup>15</sup> The target is located near the center of a through hole which passes tangentially to the core of the CP-5 research reactor located at Argonne National Laboratory. The targets for thermal capture are oxides of neodymium having masses of about 50 mg and they are contained in small graphite holders. The isotopic abundances of the two thermal-capture targets are given in Table I. A natural neodymium target having a mass of about 25 g was used for the average neutron-capture  $\gamma$ -ray experiments.

### Primary $\gamma$ -transition spectra and calibration

Comparison of thermal-neutron-capture  $\gamma$ -ray spectra from the target enriched in  $^{143}\text{Nd}$ , from the target enriched in  $^{145}\text{Nd}$ , and from the natural target allows one to make isotopic identifications with high confidence both for the primary spectra and the secondary spectra. In Fig. 2 we show examples of these thermal spectra [Figs. 2(a), 2(b), and 2(c)] for a limited energy range of the primary  $\gamma$  transitions. Also shown in Fig. 2(d) and 2(e) are

TABLE I. Neodymium isotopic abundances in the neodymium oxide targets used for thermal-neutron capture in  $^{143}\text{Nd}$ ,  $^{145}\text{Nd}$ , and natural neodymium. The average-resonance capture target contained natural neodymium. Yields in terms of the captures of thermal neutrons in an isotope for each 100 neutrons captured in *all* isotopes are listed in columns 4, 6, and 8 corresponding, respectively, to targets whose abundances are listed in columns 3, 5, and 7.

Capturing isotope	Natural target		Target $^{143}\text{Nd}$ <sup>b</sup>		Target $^{145}\text{Nd}$ <sup>b</sup>		
	Thermal $\sigma_\gamma$ <sup>a</sup>	Abundance <sup>c</sup> (%)	Yield	Enriched (%)	Yield	Enriched (%)	Yield
142	18.7 ± 0.7	27.11	10.3	2.41	0.15	1.25	0.569
143	325 ± 10	12.17	80.0	91.06	99.73	0.78	6.11
144	3.6 ± 0.3	23.85	1.7	4.43	0.054	3.62	0.32
145	42 ± 2	8.30	7.1	0.39	0.054	89.67	92.84
146	1.4 ± 0.1	17.22	0.49	1.50	0.0071	4.31	0.15
148	2.5 ± 0.2	5.73	0.28	0.14	0.0012	0.26	0.016
150	1.2 ± 0.2	5.62	0.14	0.09	0.0004	0.12	0.0034

<sup>a</sup> *Resonance Parameters*, compiled by S. F. Mughabghab and D. I. Garber, Brookhaven National Laboratory Report No. BNL-325 (National Technical Information Service, Springfield, Va., 1973), 3rd ed., Vol. I, p. c/169.

<sup>b</sup> Analysis by Oak Ridge National Laboratory where samples were purchased.

<sup>c</sup> K. Way *et al.*, Nucl. Data A5, 9 (1968).

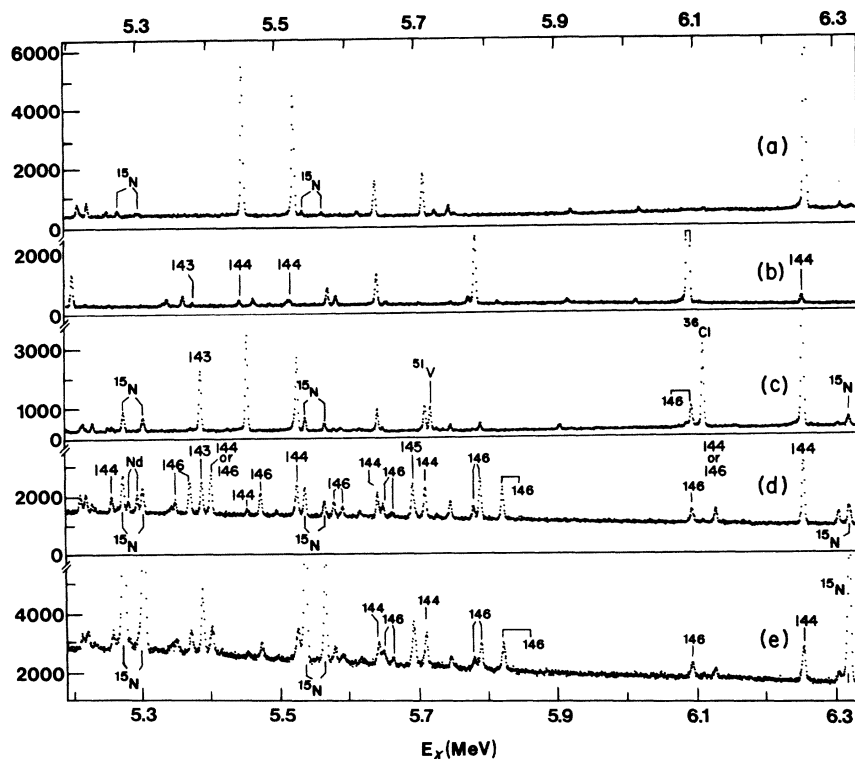


FIG. 2. Five sample spectra of  $\gamma$  transitions following neutron capture in five different neodymium targets arranged for comparison. (a) Thermal-neutron capture in a sample enriched in  $^{143}\text{Nd}$ . (b) Thermal capture in a sample enriched in  $^{146}\text{Nd}$ . (c) Thermal capture in a natural-abundance target. (d) Average-resonance neutron capture in a natural-abundance target surrounded by a 0.32-cm thick boron absorber. (e) Average-resonance neutron capture in a natural-abundance target having a 0.95-cm thick boron absorber.

two average-resonance neutron-capture  $\gamma$ -ray spectra over the same energy range. These latter two cases are obtained using boron absorbers of thicknesses 0.32 cm and 0.96 cm, respectively.

These spectra were all obtained with the spectrometer system in the coincidence mode which allows only double escape events to be recorded. Two spectra having overlapping energy range (approximately 3.6 to 5.8 MeV and 5.0 to 7.4 MeV) were obtained for each target since the 4096 channel memory capacity of the multichannel analyzer is too small to display the full-energy range of interest without losing some line definition. Line strengths compared to background are considerably less for both of the average-capture spectra [Figs. 2(d) and 2(e)] than for the thermal-capture spectra [Figs. 2(a), 2(b), and 2(c)]. This is to be expected since the neutron flux in the target material is considerably smaller in the average-capture cases compared to the flux in the surrounding materials. More massive targets are used to partially compensate for this lowered flux but this requires much larger graphite holders that scatter increased amounts of  $\gamma$  rays that come from the reactor core into the  $\gamma$ -ray beam. The

rise in background at the low-energy end of both average-capture spectra [Figs. 2(d) and 2(e)] is primarily due to the scattering of these "core"  $\gamma$  rays.

Each average-capture spectrum took about 10 days of running time; so in order to avoid loss of resolution due to electronic drift, the data were read in approximately 2-day intervals. Those runs showing no effects of drift were then added together by a computer and plotted for final analysis. Since the amplifier gain is stabilized with a precision pulser, there are seldom any drift difficulties experienced.

Energy and intensity calibrations for both thermal- and average-capture cases are based primarily on the known lines from the  $^{14}\text{N}(n, \gamma)^{15}\text{N}$  reaction.<sup>16,17</sup> To accomplish this the through tube which normally contains helium is flushed with nitrogen gas and with the target in place the calibration spectrum is collected. Another calibration spectrum is obtained with the target withdrawn in order to avoid interference between calibration and target lines and to detect any significant electronic shifts. The energies are calculated by computer using a method developed by Strauss,

Lenkszus, and Eickholz<sup>18</sup> which employs a sliding pulser to correct for the nonlinearity of the electronic system. Intensities are calculated using a computer program based on the relative intensities of the nitrogen lines listed in Table II.

The final results of the analysis of the thermal-capture  $\gamma$ -ray spectra and the average-capture  $\gamma$ -ray spectra are compiled in Tables III and IV, respectively. The analysis and tabulation of the thermal-capture data was done primarily by Hawkins<sup>19</sup> during a study of the states in  $^{144}\text{Nd}$ . The better signal-to-noise ratio, higher resolution, and enriched target in the case of the thermal spectrum allowed the analysis to be carried to lower energy (Table III) than in the case of the average-capture (Table IV) data. The  $\gamma$ -ray energies in the average-capture case were obtained with less accuracy than in the thermal case due to the poorer quality of the data. In addition there is a small energy increase for an  $M1$  line obtained from average neutron capture as compared to the same line obtained from thermal-neutron capture. This is due to the effect of the  $p$ -wave capture on the line shape in the former case. An  $E1$  line arises from a  $\gamma$  transition following pure  $s$ -wave capture only whereas an  $M1$  line following  $s$ -wave capture has an  $E1$  component due to  $p$ -wave capture which shows up primarily on the high-energy side of the line. Thus the centroid of this composite line is shifted to higher energy compared to thermal. The spectral sensitivity in the case of the average-resonance capture data is not great enough to show the detail of this composite line shape. Therefore, the energies listed in Table IV are the same as those in Table III except for those  $\gamma$  rays (listed in parentheses in Table IV) which are not observed in the thermal primary spectra. These  $\gamma$ -ray energies come from average-capture spectra and contain a 0.2–0.5-keV increase due to the higher neutron energy used in average capture compared to thermal capture.

#### Secondary $\gamma$ transitions and calibrations

With the spectrometer set to observe an energy range from 400 to 2600 keV and to reject all but full-energy detector events (anticoincidence mode) the low-energy  $\gamma$  spectra following thermal capture in three different targets ( $^{143}\text{Nd}$ ,  $^{145}\text{Nd}$ , and natural Nd) were obtained. The spectrum resulting from capture in the target enriched in  $^{145}\text{Nd}$  is shown in Fig. 3. The results are listed in Table V. Isotopic identifications were made by comparisons of our spectra and reference to papers published on the  $^{144}\text{Nd}(n, \gamma)^{145}\text{Nd}$  reaction by Hillis, Bingham, McClure, Kendrick, Hill, Raman, Ball, and Harvey<sup>20</sup> and also by Najam,

Ishaq, Anwar-ul-Islam, Khan, and Mirza<sup>21</sup>; and on the  $^{142}\text{Nd}(n, \gamma)^{143}\text{Nd}$  reaction by Mirza, Khan, Irshad, Schmidt, Ishaq, and Anwar-ul-Islam.<sup>22</sup>

The energy calibration lines used for our results are listed in Table VI. The full-energy peaks of some of the best calibration lines lie above the energy range of this data and so a special calibration spectrum with nitrogen in the through tube was taken with the coincidence mode to find accurate locations of the double escape peaks of these lines in the lower-energy range of the full-energy-peak spectrum (anticoincidence mode).

### III. RESULTS OF SPECTRAL ANALYSES

#### Primary $\gamma$ transitions

Examination of Figs. 2 (a), 2(b), and 2(c) reveals that only the strongest lines from the  $^{143}\text{Nd}(n, \gamma)^{144}\text{Nd}$  reaction [ Fig. 2(a) ] show up in the spectrum for the  $^{145}\text{Nd}(n, \gamma)^{146}\text{Nd}$  reaction [ Fig. 2(b) ] whereas not even the strongest lines from the latter show up in the former. This is consistent with the yields listed in Table I. One can see that the line marked  $^{36}\text{Cl}$  on the high-energy end of Fig. 2(c) is a contaminant of the natural-abundance target since it does not show up in average-capture spectra [ Figs. 2(d) and 2(e) ] or in enriched thermal-capture spectra [ Figs. 2(a) and 2(b) ]. It is clear also that the line next to it on the low-energy side is due to a primary transition in  $^{146}\text{Nd}$ .

Spectra obtained using natural targets exhibit highly increased complexity at an energy not far below the lower end of Fig. 2 since, in addition to the effect of increasing level densities, lines from other isotopes having lower-energy capture states begin to contribute to the spectral structure. Also the average-capture primary transitions to the first  $2^+$  states in  $^{144}\text{Nd}$  and  $^{146}\text{Nd}$  are not fully resolved from each other but this occurs at an energy above the range shown in Fig. 2.

TABLE II. Energy and intensity calibration lines for high-energy primary transitions.

$E_\gamma$ (keV)	$I_\gamma$ (%)	Reaction	Remarks
$7299.0 \pm 0.5$	10.0	$^{14}\text{N}(n, \gamma)^{15}\text{N}$	Primary standard <sup>a</sup>
$7006.3 \pm 0.3$		$^{10}\text{B}(n, \gamma)^{11}\text{B}$	Secondary standard <sup>b</sup>
$6739.0 \pm 0.3$		$^{10}\text{B}(n, \gamma)^{11}\text{B}$	Secondary standard <sup>b</sup>
$6322.0 \pm 0.4$	18.8	$^{14}\text{N}(n, \gamma)^{15}\text{N}$	Primary standard <sup>a</sup>
$5533.2 \pm 0.3$	19.7	$^{14}\text{N}(n, \gamma)^{15}\text{N}$	Secondary standard <sup>a</sup>
$5269.2 \pm 0.3$	29.1	$^{14}\text{N}(n, \gamma)^{15}\text{N}$	Primary standard <sup>a</sup>

<sup>a</sup> Reference 16.

<sup>b</sup> Reference 17.

TABLE III. Primary  $\gamma$ -ray transitions in  $^{146}\text{Nd}$  following thermal-neutron capture in  $^{145}\text{Nd}$ .  $E_L$  is the level energy and is obtained by:  $E_L = E_0 - (E_\gamma + E_\gamma^2/2mc^2)$  where  $E_0$  is the capture state energy. The latter is obtained from  $E_0 = 7110.8 + 453.7 + (7110.8)^2/2mc^2 = 7564.7$  keV. Product nuclides are used in the remarks column to identify the source of a  $\gamma$  transition.

$E_\gamma$ (keV)	$I_\gamma$	$\Delta I_\gamma/I_\gamma$ (%)	$E_L$ (keV)	Remarks
7110.8 $\pm$ 0.3	390	1.5	453.7 <sup>a</sup>	
6521.3 $\pm$ 0.4	206	2.0	1043.2	
6375.0 $\pm$ 0.3	17.0	8.0	1189.5	
6093.9 $\pm$ 0.3	314	2.2	1470.7	$^{146}\text{Nd}$ mixed with $^{14}\text{C}$
5818.3 $\pm$ 0.3	5.2	17	1746.3	
5787.4 $\pm$ 0.2	100	2.2	1777.2	
5777.4 $\pm$ 0.2	11.7	9.0	1787.2	
5752.5 $\pm$ 0.5	4.2	20	1812.1	
5645.7 $\pm$ 0.2	45.1	3.6	1918.9	
5587.5 $\pm$ 0.2	13.7	15	1977.1	
5575.3 $\pm$ 0.3	24.5	3.8	1989.3	Probably $^{146}\text{Nd}$
5492.3 $\pm$ 0.4	3.6	19	2073.0	
5468.7 $\pm$ 0.3	10.2	7.4	2095.9	
5367.3 $\pm$ 0.3	15.6	5.5	2197.3	$^{146}\text{Nd}$ ; may have some $^{144}\text{Nd}$
5344.8 $\pm$ 0.3	11.6	7.5	2219.8	
5338.2 $\pm$ 0.3	5.5	16	2226.4	Probably $^{146}\text{Nd}$
5207.6 $\pm$ 0.2	47.8	2.7	2357.0	
5131.0 $\pm$ 0.5	3.1	26	2433.6	
5128.2 $\pm$ 0.3	7.5	9.9	2436.4	Probably $^{146}\text{Nd}$
5125.8 $\pm$ 0.3	3.4	20	2438.8	
5094.7 $\pm$ 0.3	10.3	7.7	2469.9	
5073.2 $\pm$ 0.3	11.5	6.7	2491.4	
5048.3 $\pm$ 0.3	24.7	4.2	2516.3	
5043.3 $\pm$ 0.3	39.6	3.2	2521.3	
5036.3 $\pm$ 0.3	6.7	12	2528.3	
5011.9 $\pm$ 0.2	76.4	2.1	2552.7	
5002.5 $\pm$ 0.3	14.0	6.4	2562.2	
4990.9 $\pm$ 0.3	5.4	14	2573.7	
4975.1 $\pm$ 0.3	29.4	3.7	2589.5	
4903.8 $\pm$ 0.3	5.2	15	2660.8	
4857.3 $\pm$ 0.3	4.3	18	2707.3	$^{146}\text{Nd}$ ; may have some $^{144}\text{Nd}$
4814.5 $\pm$ 0.2	26.7	4.2	2750.1	
4780.8 $\pm$ 0.3	10.1	8.5	2783.8	
4720.0 <sup>b</sup> $\pm$ 0.3	4.2	19	2844.6	
4694.0 <sup>b</sup> $\pm$ 0.3	2.2	35	2870.6	$^{146}\text{Nd}$ most likely
4679.3 <sup>b</sup> $\pm$ 0.3	5.2	20	2885.3	
4634.0 $\pm$ 0.2	22.7	5.0	2930.6	
4595.0 <sup>b</sup> $\pm$ 0.3	6.4	15	2969.6	
4567.9 $\pm$ 0.2	46.9	3.0	2996.7	
4551.4 $\pm$ 0.5	5.6	30	3013.2	
4473.4 <sup>b</sup> $\pm$ 0.3	5.7	$\pm$ 15	3091.2	

<sup>a</sup> This level value obtained from the first  $2^+$  to  $0^+$  ground-state transition whose energy is obtained from the low-energy anticoincidence data.

<sup>b</sup> Not evident in average-capture spectra either because the intensity is lost in a multiplet structure or is below sensitivity in this energy range.

Comparison of Fig. 2 (d) with Fig. 2(e) reveals that the former has higher resolution as expected with the thinner boron absorber. In addition, the relative intensities have changed significantly in some cases because of averaging over a different set of neutron resonances. The reduced relative intensities,  $I_\gamma(E_0/E_\gamma)^3$ , obtained from the average capture with a 0.95-cm boron ab-

sorber [ Fig. 2(e) ] are shown in Fig. 4. A similar plot of the reduced intensities obtained from the average capture with a 0.32-cm boron absorber did not reveal as clear a delineation between spin-parity groups as is obtained with the data taken using the 0.95-cm absorber because of poorer averaging of the Porter-Thomas fluctuations that occurs when too few resonances are used.

TABLE IV. Primary  $\gamma$ -ray transitions in  $^{146}\text{Nd}$  following average-resonance neutron capture in the natural-abundance neodymium oxide target surrounded by a 0.95-cm thick boron absorber. Energies under the  $E_\gamma$  column are obtained from the calibration of the thermal-capture primary  $\gamma$ -transition spectrum, except in the cases shown in parentheses which come from average-capture data only. The level values in column 3 are those appearing in the final level scheme and similarly for the  $J^\pi$  assignments in column 5.

$E_\gamma$ (keV)	$I_\gamma \left(\frac{E_0}{E_\gamma}\right)^3$	$\frac{\Delta I_\gamma}{I_\gamma}$ (%)	$E_L$ (keV)	Multipole	$J^\pi$	Remarks
7110.8 $\pm$ 0.3	5.5	12	453.7	E1	2 <sup>+</sup>	a
6521.3 $\pm$ 0.4	17.6	6	1043.1	E1	4 <sup>+</sup>	a
6375.0 $\pm$ 0.3	1.6	29	1189.6	M1	3 <sup>-</sup>	a
...	...		1377.1	M1	1 <sup>-</sup>	b
6093.9 $\pm$ 0.3	5.7	11	1470.2	E1	2 <sup>+</sup>	a
5818.3 $\pm$ 0.3	10.7	7	1745.4	E1	3 <sup>+</sup> , 4 <sup>+</sup>	
5787.4 $\pm$ 0.2	10.0	7	1777.7	E1	3 <sup>+</sup> , 4 <sup>+</sup>	
5777.4 $\pm$ 0.2	4.7	14	1787.8	E1	2 <sup>+</sup>	a
5752.5 $\pm$ 0.5	0.81	80	1812.1	M1	2 <sup>-</sup> , 5 <sup>-</sup> (3 <sup>-</sup> , 4 <sup>-</sup> )	
(5680.0 $\pm$ 0.5) <sup>c</sup>	0.86	83	1884.7 <sup>d</sup>	M1	2 <sup>-</sup> , 5 <sup>-</sup> (3 <sup>-</sup> , 4 <sup>-</sup> )	
(5669.1 $\pm$ 1.0) <sup>c</sup>	0.43	100		M1 or E2		
5645.7 $\pm$ 0.2	5.3	12	1919.1	E1	2 <sup>+</sup>	a
5587.5 $\pm$ 0.2	3.4	20	1978.4	E1	2 <sup>+</sup>	a
5575.3 $\pm$ 0.3	5.6	13	1989.5	E1	2 <sup>+</sup>	a
5492.3 $\pm$ 0.4	1.4	85	2073.0	M1	3 <sup>-</sup> , 4 <sup>-</sup> (2 <sup>-</sup> , 5 <sup>-</sup> )	
5468.7 $\pm$ 0.3	6.2	13	2096.3	E1	2 <sup>+</sup> , 5 <sup>+</sup> (3 <sup>+</sup> , 4 <sup>+</sup> )	
5367.3 $\pm$ 0.3	9.5	10	2197.3	E1	3 <sup>+</sup> , 4 <sup>+</sup>	
5344.8 $\pm$ 0.5	5.0	17	2220.1	E1	2 <sup>+</sup>	
5338.2 $\pm$ 0.5	4.2	22	2226.4	E1	2 <sup>+</sup> , 5 <sup>+</sup>	
(5333.7 $\pm$ 0.7) <sup>c</sup>	1.8	50	2231.0	M1	3 <sup>-</sup> , 4 <sup>-</sup> (2 <sup>-</sup> , 5 <sup>-</sup> )	
(5277.6 $\pm$ 0.6) <sup>c</sup>	5.1	18	2286.9	E1	2 <sup>+</sup> , 5 <sup>+</sup>	
(5262.6 $\pm$ 0.5) <sup>c</sup>	4.7	21	2302.0 <sup>d</sup>	E1	2 <sup>+</sup> , 5 <sup>+</sup>	
5207.6 $\pm$ 0.2	5.8	17	2357.0	E1	2 <sup>+</sup> , 5 <sup>+</sup> (3 <sup>+</sup> , 4 <sup>+</sup> )	
(5145.3 $\pm$ 0.3) <sup>c</sup>	4.9	22	2419.4	E1	2 <sup>+</sup> , 5 <sup>+</sup>	
5131.0 $\pm$ 0.5	1.7	61	2433.6	M1	3 <sup>-</sup> , 4 <sup>-</sup> (2 <sup>-</sup> , 5 <sup>-</sup> )	
5128.2 $\pm$ 0.5	4.5	25	2435.5	E1	2 <sup>+</sup> , 5 <sup>+</sup>	
5125.8 $\pm$ 0.5	4.3	26	2438.0	E1	2 <sup>+</sup> , 5 <sup>+</sup>	
5094.7 $\pm$ 0.3	6.0	19	2469.8	E1	2 <sup>+</sup> , 5 <sup>+</sup> (3 <sup>+</sup> , 4 <sup>+</sup> )	
(5079.3 $\pm$ 0.5) <sup>c</sup>	5.8	20	2483.7	E1	2 <sup>+</sup> , 5 <sup>+</sup>	e
5073.2 $\pm$ 0.5	6.5	18	2491.6	E1	2 <sup>+</sup> , 5 <sup>+</sup> (3 <sup>+</sup> , 4 <sup>+</sup> )	
5048.3 $\pm$ 0.3	0.9	62	2516.3	M1	2 <sup>-</sup> , 5 <sup>-</sup> (3 <sup>-</sup> , 4 <sup>-</sup> )	
5043.3 $\pm$ 0.4	4.5	26	2521.8	E1	2 <sup>+</sup> , 5 <sup>+</sup>	
5036.3 $\pm$ 0.3	5.3	22	2528.3	E1	2 <sup>+</sup> , 5 <sup>+</sup>	
(5016.9 $\pm$ 0.4) <sup>c</sup>	5.7	20	2547.8	E1	2 <sup>+</sup> , 5 <sup>+</sup>	f, g
5011.9 $\pm$ 0.2	6.7	15	2552.2	E1	2 <sup>+</sup> , 5 <sup>+</sup>	
(5008.7 $\pm$ 0.3) <sup>c</sup>	9.2	10	2556.0	E1	3 <sup>+</sup> , 4 <sup>+</sup>	f, g
5002.5 $\pm$ 0.5	5.3	20	2562.2	E1	2 <sup>+</sup> , 5 <sup>+</sup>	
4990.9 $\pm$ 0.3	10.3	8	2573.7	E1	3 <sup>+</sup> , 4 <sup>+</sup>	Possible doublet <sup>g</sup>
4975.1 $\pm$ 0.3	12.0	20	2589.6	E1	3 <sup>+</sup> , 4 <sup>+</sup>	h
(4963.1 $\pm$ 0.6)	1.5	76	2601	M1	3 <sup>-</sup> , 4 <sup>-</sup> (2 <sup>-</sup> , 5 <sup>-</sup> )	
4903.8 $\pm$ 0.3	10.0	10	2660.9	E1	3 <sup>+</sup> , 4 <sup>+</sup>	Possible doublet
4857.5 $\pm$ 0.5	7.0	20	2706.3	E1	3 <sup>+</sup> , 4 <sup>+</sup>	g
4814.5 $\pm$ 0.5	5.2	25	2749.3	E1	2 <sup>+</sup> , 5 <sup>+</sup>	g
4780.8 $\pm$ 0.4	8.2	15	2783.5	E1	3 <sup>+</sup> , 4 <sup>+</sup>	g
(4761.6 $\pm$ 0.5) <sup>c</sup>	10.6	15	2803.1	E1	3 <sup>+</sup> , 4 <sup>+</sup>	g
4658.9 $\pm$ 0.6	6.2	25	2905.8	E1	3 <sup>+</sup> , 4 <sup>+</sup> , 2 <sup>+</sup> , 5 <sup>+</sup>	g
4634.0 $\pm$ 0.5	6.0	20	2930.6	E1	3 <sup>+</sup> , 4 <sup>+</sup> , 2 <sup>+</sup> , 5 <sup>+</sup>	g
(4606.1 $\pm$ 0.5) <sup>c</sup>	5.5	25	2958.6	E1	3 <sup>+</sup> , 4 <sup>+</sup> , 2 <sup>+</sup> , 5 <sup>+</sup>	f, g
4567.9 $\pm$ 0.5	7.1	21	2996.8	E1	3 <sup>+</sup> , 4 <sup>+</sup>	g
4551.4 $\pm$ 0.4	8.2	18	3013.3	E1	3 <sup>+</sup> , 4 <sup>+</sup>	g
(4530.0 $\pm$ 0.5) <sup>c</sup>	5.0	30	3034.7	E1	3 <sup>+</sup> , 4 <sup>+</sup> (2 <sup>+</sup> , 5 <sup>+</sup> )	f, g
(4522.4 $\pm$ 0.5) <sup>c</sup>	6.7	23	3042.3	E1	3 <sup>+</sup> , 4 <sup>+</sup>	g
(4500.0 $\pm$ 0.5) <sup>c</sup>	6.7	23	3064.7	E1	3 <sup>+</sup> , 4 <sup>+</sup>	f, g
(4392.6 $\pm$ 0.5) <sup>c</sup>	7.2	22	3172.1	E1	3 <sup>+</sup> , 4 <sup>+</sup>	f, g

TABLE IV (Continued)

$E_\gamma$ (keV)	$I_\gamma \frac{E_0}{E_\gamma}^3$	$\frac{\Delta I_\gamma}{I_\gamma}$ (%)	$E_L$ (keV)	Multipole	$J^\pi$	Remarks
$(4386.4 \pm 0.5)^c$	5.8	25	3178.3	E1	$3^+, 4^+, 2^+, 5^+$	g
$(4334.9 \pm 0.4)^c$	8.0	20	3229.8	E1	$3^+, 4^+$	f, g

<sup>a</sup> The other spin choice suggested by the primary-transition intensity is ruled out by low-energy transitions connected to this state or by the work of other authors (see level scheme discussion).

<sup>b</sup> Evidence for this level is found in past literature and/or in our low-energy spectrum (see discussion of levels).

<sup>c</sup> Energy based on average-resonance neutron-capture data using the 0.32-cm boron absorber. These energies are shifted up by 0.2–0.5 keV from the thermal values.

<sup>d</sup> Level energy is based on average-resonance neutron-capture data using the 0.32-cm boron absorber. These level energies are shifted down by 0.2–0.5 keV from the level energies based on the thermal-capture data.

<sup>e</sup> Three major components of what might be six lines.

<sup>f</sup> Observed in both average-capture runs only; energy listed comes from thin-absorber spectrum.

<sup>g</sup> Uncertain isotopic identification.

<sup>h</sup> Only half the observed intensity is listed, the other half is assigned to  $^{144}\text{Nd}(n, \gamma)^{145}\text{Nd}$ .

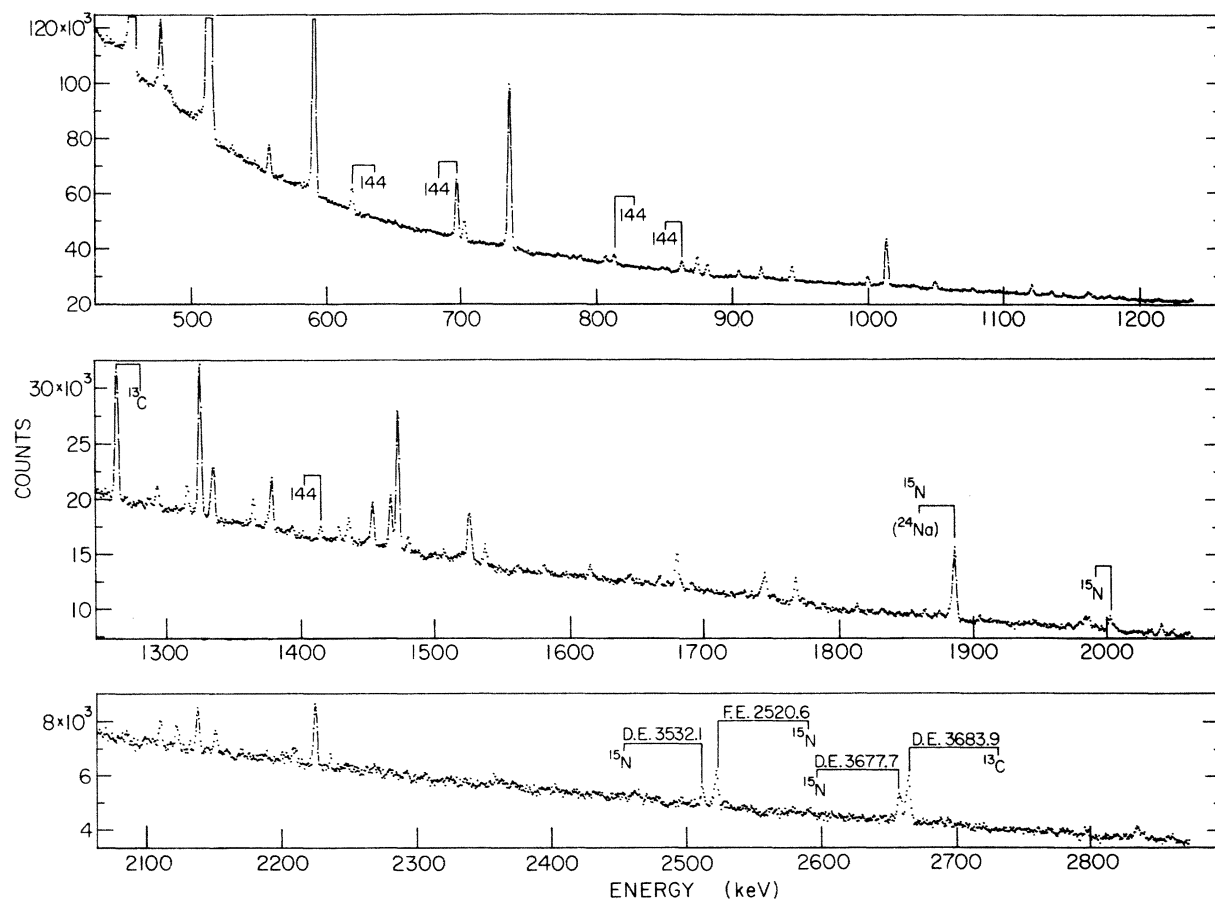


FIG. 3. Spectrum of low-energy  $\gamma$  rays following thermal capture in a target enriched in  $^{146}\text{Nd}$ .

TABLE V. Secondary  $\gamma$  transitions following  $^{145}\text{Nd}(n,\gamma)^{146}\text{Nd}$  as measured with an intrinsic-germanium detector. The target is enriched to 89.7%  $^{145}\text{Nd}$ .  $I_\gamma$  is the relative intensity normalized to the 453.7-keV  $\gamma$  ray whose intensity is arbitrarily set to 100. The dagger in column 2 indicates that the line appears; the double dagger under column 2 indicates that the line appears in the level scheme twice.

$E_\gamma$ (keV)	In scheme	$I_\gamma$	$\frac{\Delta I_\gamma}{I_\gamma} \times 100^a$ (%)	Remarks
448.4±0.6	††	1.1	18	
453.7±0.1	†	100.0	0.2	
467.4±0.7		0.16	83	
471.4±0.6		0.70	30	
474.5±0.2	†	7.5	1.9	
476.7±0.5		0.62	25	} Doublet may contain 478-keV $^{144}\text{Nd}$ $\gamma$ ray
479.2±0.5		0.83	20	
482.0±0.5		0.74	20	
522.9±0.6		0.30	25	
528.3±0.4	†	0.56	14	} Possible decay from a 1915 <sup>c</sup> state to 1 <sup>-</sup> at 1377 keV
534.9±0.6		0.25	30	
545.4±0.6		0.20	36	
555.9±0.2	†	2.4	2.9	
565.1±0.6		0.25	25	
578.0±0.5		0.29	19	
584.6±0.6		0.32	17	
589.4±0.2	†	27.0	0.4	} Weak multiplet in wing of 589.4-keV line
598.3±0.5	†	0.34	16	
600.0±0.8		0.12	50	
602.0±0.8	†	0.12	50	
630.1±0.5		0.17	29	
650.6±0.5	†	0.29	18	
674.3±0.4		0.10	50	
677.1±0.5		0.10	50	
702.1±0.2	†	1.7	3	} Doublet with $^{144}\text{Nd}$ ; <sup>d</sup>
716.8±0.5	†	0.17	29	
721.6±0.5		0.07	63	} e
724.6±0.4	†	0.22	22	
729.6±0.5	†	0.25	20	
735.9±0.2	†	15.3	0.5	} Doublet with $^{143}\text{Nd}$ ; <sup>d</sup>
745.2±0.4	†	0.16	30	
757.7±0.5		0.15	32	
765.1±0.5		0.12	37	
772.5±0.2		0.39	12	
775.6±0.5	†	0.37	12	
788.8±0.3	†	0.43	11	
807.3±0.2		0.70	6.9	
849.9±0.3		0.31	15	
868.5±0.4		0.26	18	
871.5±0.4		0.34	14	
875.9±0.2	†	1.7	2.9	} Possible doublet
883.3±0.2		1.1	5	
906.7±0.2	†	0.65	7	
923.2±0.2	†	1.1	5	
946.3±0.2	†	1.5	4	
1002.7±0.2		0.84	6	
1012.3±0.4		0.22	21	
1016.9±0.2	†	4.7	1.3	
1029.6±0.3	††	0.17	28	
1036.8±0.3	†	0.25	19	
1039.5±0.3		0.16	30	
1053.1±0.2	†	0.78	6	} Possible doublet



TABLE V (Continued)

$E_\gamma$ (keV)	In scheme	$I_\gamma$	$\frac{\Delta I_\gamma}{I_\gamma} \times 100^a$ (%)	Remarks
1081.1 ± 0.2		0.34	13	Possible decay from $2^-$ state at 1.534 <sup>c</sup>
1093.5 ± 0.3		0.14	32	
1125.1 ± 0.2		1.0	5	Doublet with $^{144}\text{Nd}^f$
1139.9 ± 0.2		0.48	10	
1149.8 ± 0.4		0.21	22	
1165.2 ± 0.5		0.12	38	
1167.2 ± 0.2	†	0.64	7	
1169.5 ± 0.4		0.30	15	
1181.7 ± 0.4		0.15	31	
1183.6 ± 0.4	†	0.24	19	
1190.8 ± 0.4		0.30	15	
1193.4 ± 0.4		0.31	19	
1219.9 ± 0.4		0.22	21	
1244.0 ± 0.4	††	0.22	20	
1268.5 ± 0.4		0.22	20	
1292.2 ± 0.3	†	0.64	7	
1314.3 ± 0.3	†	0.79	7	
1324.0 ± 0.3	†	3.4	1.7	
1332.3 ± 0.4	†	0.26	18	Close doublet
1333.9 ± 0.3	†	1.5	4	
1363.5 ± 0.3		0.79	6	
1377.3 ± 0.3	†	1.6	3	
1382.0 ± 0.5		0.1	45	
1392.3 ± 0.3	†	0.27	17	
1426.5 ± 0.3	†	0.41	11	
1434.3 ± 0.3		0.79	6	
1448.6 ± 0.4	†	0.24	19	
1452.2 ± 0.3		1.4	4	
1465.4 ± 0.3	†	1.8	3	
1468.8 ± 0.3		0.30	17	
1471.0 ± 0.3	†	4.4	1.3	
1478.6 ± 0.3	†	0.45	10	
1496.5 ± 0.4		0.11	40	
1502.9 ± 0.4		0.22	20	
1521.9 ± 0.3		1.3	4	Triplet with $^{144}\text{Nd}$ line
1525.5 ± 0.5	†	0.90	5	
1536.0 ± 0.3	†	0.66	7	
1560.1 ± 0.3		0.29	15	
1579.5 ± 0.4		0.34	13	
1613.9 ± 0.3		0.49	9	
1637.8 ± 0.6		0.23	19	
1665.6 ± 0.3		0.33	13	
1671.8 ± 0.4		0.19	23	d
1680.9 ± 0.4		0.31	14	
1689.8 ± 0.4		0.31	14	
1728.4 ± 0.5		0.20	22	
1741.4 ± 0.3		0.48	10	
1744.3 ± 0.3	†	1.0	5	
1750.7 ± 0.3		0.32	14	
1766.7 ± 0.2	†	1.0	5	e
1771.1 ± 0.3		0.16	26	
1777.3 ± 0.3		0.12	35	
1779.8 ± 0.3		0.12	35	
1787.3 ± 0.3	†	0.17	23	
1812.1 ± 0.3		0.29	15	
1832.9 ± 0.3	†	0.25	17	

TABLE V (Continued)

$E_\gamma$ (keV)	In scheme	$I_\gamma$	$\frac{\Delta I_\gamma}{I_\gamma} \times 100^a$ (%)	Remarks
1853.3 ± 0.3		0.25	17	
1862.7 ± 0.3		0.34	13	
1873.5 ± 0.4		0.24	18	
1880.5 ± 0.5		0.21	15	
1903.2 ± 0.4	†	0.31	15	
1906.8 ± 0.6		0.09	50	
1910.8 ± 0.6		0.09	50	
1914.1 ± 0.6		0.10	45	
1917.4 ± 1.0		0.06	80	
1919.7 ± 1.0		0.07	80	
1944.2 ± 0.3		0.15	30	
1969.0 ± 0.5		0.16	40	Possible doublet
1975.1 ± 0.5		0.11	60	
1977.7 ± 0.5		0.23	50	
1981.4 ± 0.3	†	0.42	20	
1984.2 ± 0.4	†	0.43	20	
1989.2 ± 0.5	†	0.18	60	
2003.0 ± 0.3	†	0.16	30	
2030.0 ± 0.3	†	0.18	25	
2037.8 ± 0.3	†	0.46	10	
2045.6 ± 0.3		0.17	25	
2057.8 ± 0.3		0.18	25	
2083.2 ± 0.3		0.20	20	
2096.3 ± 1.0		0.10	50	
2108.3 ± 0.2		0.46	9	
2120.2 ± 0.3		0.38	11	
2136.0 ± 0.2		0.71	6	
2142.5 ± 0.5		0.10	43	
2149.1 ± 0.3		0.31	13	
2157.6 ± 1.0		0.07	60	
2168.5 ± 0.3		0.13	33	
2207.0 ± 0.3		0.23	19	
2209.4 ± 0.3		0.23	19	
2223.5 ± 0.2		1.3	4	
2234.5 ± 0.3		0.21	20	
2266.8 ± 0.3		0.17	24	
2278.1 ± 0.3		0.10	40	
2291.2 ± 0.3		0.13	31	
2369.5 ± 0.3		0.12	33	
2459.8 ± 0.3		0.14	30	
2658.9 ± 0.4		0.20	20	
2685.6 ± 0.3		0.15	31	
2691.3 ± 0.3		0.13	33	
2793.0 ± 0.4		0.14	29	
2830.3 ± 0.5		0.24	18	
2852.8 ± 0.4		0.12	36	
2856.5 ± 0.4		0.23	19	

<sup>a</sup> This error is based on the total accumulated counts in the center of the peak where  $\Delta I_\gamma = (\sigma^2 + \sigma_b^2)^{1/2}$  with  $\sigma^2$  being the variance of the total peak count and  $\sigma_b^2$  the variance of the background under the peak. The contributions to the relative intensity error due to errors in the linewidth, efficiency, and transmission are at most 2%, 10%, and 15%, respectively, up to 1500 keV. Above 1500 keV the efficiency error is at most 20%.

<sup>b</sup> Although identifiable numerical intensity ratios have not been established between two spectra using targets enriched in  $^{143}\text{Nd}$  and  $^{145}\text{Nd}$  for all of the listed  $\gamma$  rays, we have been able to establish which lines from competing isotopes can give intensities above our threshold

TABLE V (Continued)

of sensitivity. This allows us to assign the rest of the lines to transitions in  $^{146}\text{Nd}$  to high probability.

<sup>c</sup> Reference 4.

<sup>d</sup> Unfolded from a stronger line of the designated isotope or from a stronger line of unknown origin if no designation is given.

<sup>e</sup> Another line may be present in this multiplet structure.

<sup>f</sup> Unfolded from a weaker line of the designated isotope.

The excessive intensity of the primary transition to the  $4^+$  state at 1043 keV is probably due to the effect of a few strong low-energy neutron resonances with large  $\gamma$ -ray widths. We have no evidence that the spectral line for this state is a doublet but the possibility is considered in regard to a state proposed by Berzin *et al.*<sup>10</sup> in the discussion of the level scheme.

The essentially horizontal pair of guidelines superimposed on the  $E1$  transitions are spaced to give a 2 to 1 intensity ratio. The same slope was used for the  $M1$  guidelines since the uncertainties in the  $M1$  intensities prevented the independent determination of a slope for  $M1$  radiation. The data are at least consistent with the  $E1$  slope. The  $E1$  intensities are about 6 times greater than the  $M1$  intensities consistent with the expectations reported by Bollinger and Thomas.<sup>13</sup> The point of lowest intensity is 100% uncertain in magnitude

TABLE VI. Calibration lines for the medium-energy spectrum. Except for the first line listed, all calibration lines come from the  $^{14}\text{N}(n, \gamma)^{15}\text{N}$  reaction. The double-escape peaks of the  $^{15}\text{N}$  lines are used to calibrate the full-energy peaks of the  $^{146}\text{Nd}$  lines so the corresponding detector energies are listed in column 2. The two primary standards were used with the ramp-generator technique to obtain the calibration of the spectrum by use of a computer. The secondary standards provided a check on the success of the calibration and means for preliminary hand calculations.

$E_\gamma$ <sup>a</sup> (keV)	Detector energy (keV) $E_\gamma - 2mc^2$	Remarks
$1261.92 \pm 0.06$ <sup>b</sup>		Secondary standard
$1884.81 \pm 0.10$	$862.81 \pm 0.06$	Primary standard
$1999.65 \pm 0.10$	$977.65 \pm 0.10$	Secondary standard
$2520.55 \pm 0.10$	$1498.55 \pm 0.10$	Secondary standard
$2831.1 \pm 0.2$	$1809.1 \pm 0.2$	Secondary standard
$3532.2 \pm 0.2$	$2510.2 \pm 0.2$	Primary standard
$3677.7 \pm 0.2$	$2655.7 \pm 0.2$	Secondary standard

<sup>a</sup> The energy values for the  $\gamma$  rays from the  $^{14}\text{N}(n, \gamma)^{15}\text{N}$  reaction were obtained from R. C. Greenwood (Ref. 16).

<sup>b</sup> This line comes from the  $^{12}\text{C}(n, \gamma)^{13}\text{C}$  reaction and the value comes from W. V. Prestwich, R. E. Cote', and G. E. Thomas, Phys. Rev. Vol 161, 1080 (1967).

and represents a possible state at 1896 keV populated by a 5669-keV primary  $\gamma$  ray. The existence and isotopic assignment for this line are too uncertain to include the state in the level scheme.

#### Capture state

There is evidence that thermal neutrons produce  $3^-$  capture states much more often than  $4^-$  capture states whereas average-capture produces about equal numbers of each. As a result of thermal-neutron capture in  $^{145}\text{Nd}$ , we observe a strong primary transition to the first  $2^+$  state (Table III) in  $^{146}\text{Nd}$  as do Groshev *et al.*<sup>9</sup> and Reddingius *et al.*<sup>11</sup> Each of the two lowest-energy resonances have a spin value of  $3^-$ .<sup>14</sup> Groshev *et al.*<sup>9</sup> have pointed out that the cross section for thermal capture is relatively large so that with the above information there are grounds to assume that thermal-neutron capture favors  $3^-$  as stated above. This is also consistent with the fact that we have observed generally strong  $E1$  primary transitions to the  $2^+$  and  $4^+$  states in both  $^{144}\text{Nd}$  and  $^{146}\text{Nd}$  for the case of thermal-neutron capture. One notable exception occurs in the case of the first  $2^+$  state in  $^{144}\text{Nd}$  for which a

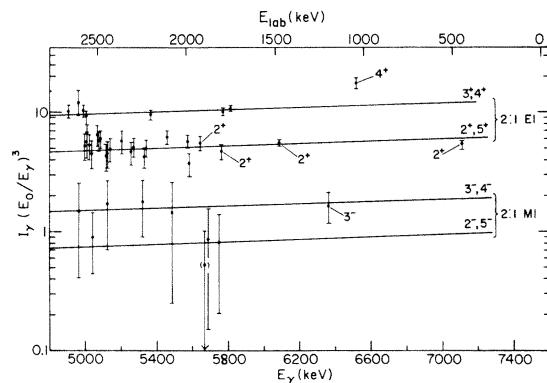


FIG. 4. Plot of the reduced  $\gamma$ -ray intensities for primary transitions in  $^{146}\text{Nd}$  following average-resonance neutron capture in a natural-abundance target surrounded by 0.95 cm of boron absorber. Each pair of straight lines drawn for both the  $E1$  and  $M1$  intensity groups is separated to give an intensity ratio of 2 as suggested by the selection rules.

primary transition is not observed in our thermal-neutron-capture  $\gamma$ -ray spectrum.

The capture-state energy is obtained using the relation  $E_0 = E_\gamma + E_L + (E_\gamma)^2/2mc^2$  where  $E_L$  is the energy of the final state to which the primary transition goes,  $E_\gamma$  is the energy of the emitted primary photon, and the last term is the recoil energy. When this is applied to the four highest-energy primary transitions (obtained from thermal-neutron capture) to the final states at 453.7 keV ( $2^+$ ), 1043.1 keV ( $4^+$ ), 1189.6 keV ( $3^-$ ), and 1470.8 keV ( $2^+$ ) one obtains an average  $E_0$  of 7564.71 keV with an rms deviation of  $\pm 0.11$  keV among the four resulting energies. The rms error must be accidentally small since the  $\gamma$ -ray random errors are at best 0.3 keV. We feel that 7564.7  $\pm 0.2$  keV is the best value based on our data. A systematic error of about 0.3 keV is possible since the average  $E_0$  based on the seventh, eighth, and tenth states is  $7565.0 \pm 0.2$ . A 0.3-keV systematic error could easily arise from a systematic error in the energy values for the nitrogen calibration lines (see Table II).

#### IV. LEVEL SCHEME DISCUSSION

##### Construction and general features

The procedure used to develop the level scheme (Fig. 5) is as follows:

(1) Each average-capture primary  $\gamma$  transition (Table IV) is used to predict the existence of a level having spin and parity suggested by the intensity of the transition. The best preliminary estimate of the level energy is obtained by  $E_L = E_0 - E_\gamma - E_R$  where in left to right sequence the energies are, level energy, capture-state energy, thermal primary  $\gamma$ -ray energy, and recoil energy. (See Table III.)

(2) Possible secondary  $\gamma$  transitions between the levels are determined by calculating energy-level differences.

(3) The  $J^\pi$  assignments of the well established low-lying levels are made use of in determining which low-energy fits can most reasonably be retained in the level scheme. These low-energy  $\gamma$ -ray fits may then make it possible to select the most probable choice of spin from among the possibilities indicated by the average-neutron-capture data and also to determine a more accurate level energy.

The resulting level scheme for  $^{146}\text{Nd}$  (Fig. 5) has average-neutron-capture primary transitions (see Table IV) shown depopulating the capture states with energies obtained from corresponding transitions produced with thermal-neutron capture (Table II) shown at the top of the figure. Where a thermal primary transition is not available the

energy measured for the primary line from average-neutron capture is shown in parenthesis. The appropriate energy shift correction should be applied to these energies to calculate energy level differences.

##### Levels to 1470.8 keV

We have obtained evidence for five excited states up to and including the 1470.8-keV  $2^+$  state (see Fig. 5). In four cases (453.7 keV,  $2^+$ ; 1043.1 keV,  $4^+$ ; 1189.6 keV,  $3^-$ ; and 1470.8 keV,  $2^+$ ) we observe primary transitions from the capture state following average-resonance neutron capture in  $^{145}\text{Nd}$ . For all five states including the  $1^-$  state at 1377.1 keV we have observed low-energy  $\gamma$  transitions. These results are consistent with the results of the  $^{146}\text{Pm}$   $\beta$ -decay work of Buss *et al.*<sup>3</sup> and Taylor *et al.*<sup>4</sup> where the first three excited states are fed; however, we have no evidence for the existence of the level at 1233 keV tentatively suggested by Buss *et al.*<sup>3</sup> All five states are reported by Oakey *et al.*<sup>6</sup> using  $\alpha$  decay from  $^{150}\text{Sm}$  but with no  $J^\pi$  assignments for the 1380- and 1473-keV states. Daniels *et al.*<sup>1</sup> report all five levels with the addition of a tentative 1224-keV state; however, they have made no  $J^\pi$  assignments for either the 1224- or 1470-keV states. The neutron-capture  $\gamma$ -ray study by Berzin *et al.*<sup>10</sup> makes use of conversion electron spectra to suggest eight states where they not only include the 1224-keV state (no  $J^\pi$  assignment) reported by Daniels *et al.*,<sup>1</sup> but also a possible  $0^+$  state at 999.1 keV and a tentative state at 1049.1 keV. They offer the speculation that these last two states are members of a two-phonon triplet so that the 1049.1-keV level would be expected to have  $J^\pi = 2^+$ . Berzin *et al.*<sup>10</sup> suggest that the 6-keV separation from the 1043-keV state leads to an unresolved doublet in the primary ( $n, \gamma$ ) spectra of Groshev *et al.*<sup>9</sup> and of Reddingius.<sup>12</sup> Reference to Fig. 4 shows that the intensity of the 6521.3-keV primary transition to the 1043.1-keV  $4^+$  state is larger than expected. If one assumes that the 6521.3-keV line is a combination of two  $E1$  transitions that proceed to a  $4^+$  state and a  $2^+$  then their intensities can be chosen so that they have the expected 2 to 1 ratio and will still be consistent with the average intensities observed for the two  $E1$  groups in Fig. 4. The intensity of a very small, contaminant line from the reaction  $^{51}\text{V}(n, \gamma)^{52}\text{V}$  (about 2% of the listed 6521.3 intensity) has been removed from the intensity of the Nd line. If there are two states, they must be less than 6 keV apart (the separation suggested by Berzin *et al.*<sup>10</sup>) since the primary-transition linewidth is at most only a few percent

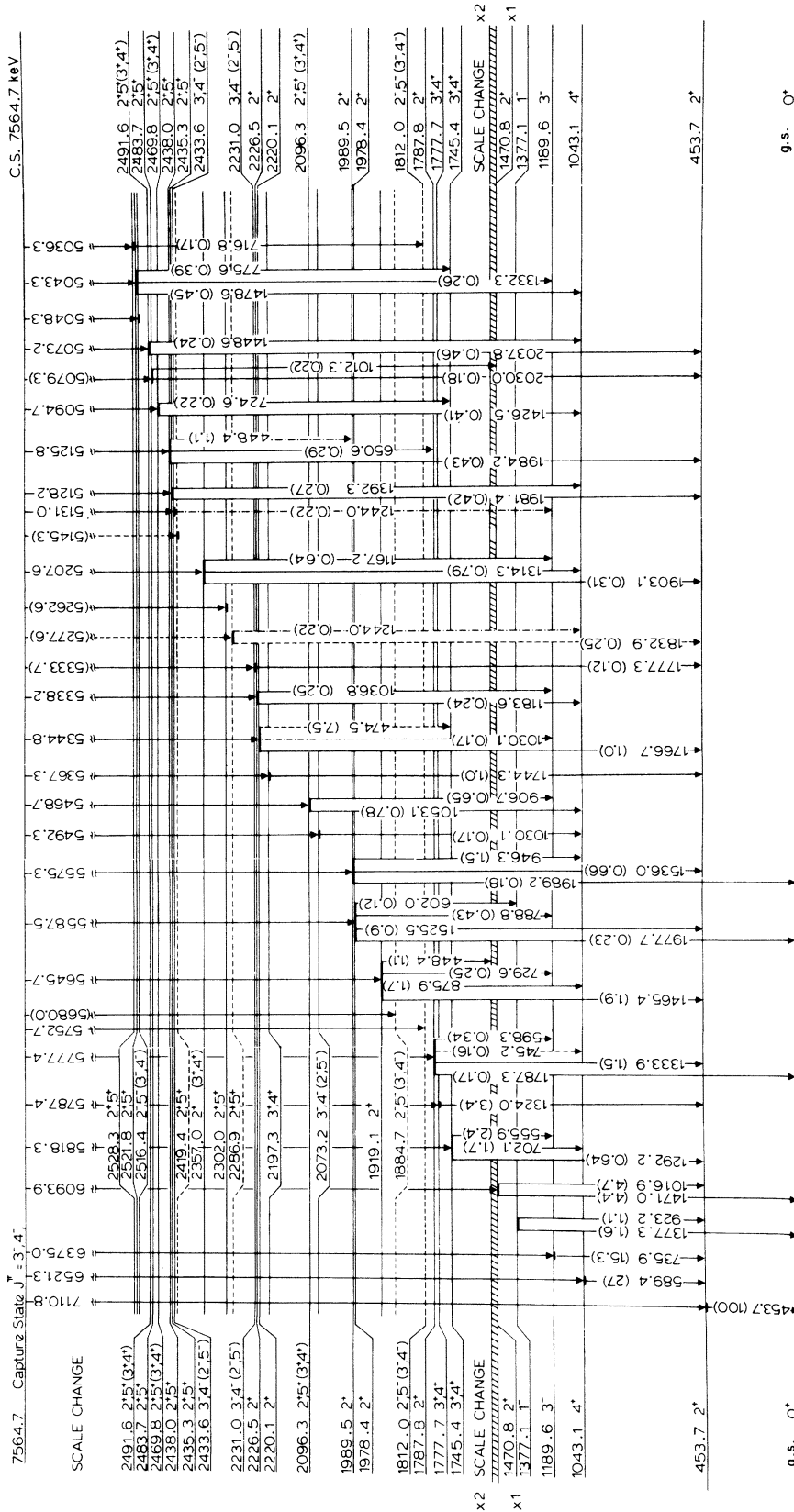


FIG. 5. Partial level scheme for  $^{146}\text{Nd}$  based on neutron-capture  $\gamma$ -ray spectroscopy. A transition shown with a dot-dash line is located twice in the level scheme. A dash line depicts a special intensity problem or marginal energy fit. A pair of  $J^\pi$  values in parentheses indicates a less favored choice which nevertheless cannot be ruled out. A primary  $\gamma$ -ray energy listed along the top of the diagram in parentheses means the energy was not available from thermal capture so the average-capture value is adopted for the diagram. The corresponding thermal-capture transitions will be 0.2–0.5 keV lower in energy. A dashed level implies marginal evidence for its existence.

greater than the linewidths for the first and second  $2^+$  states. We are not able to observe line broadening if two lines of intensity ratio 2:1 are within 2 keV of each other. The average-capture spectrum using a 0.32-cm thick boron absorber [Fig. 4(d)] has better resolution than in the case of the spectrum using a 0.95-cm thick boron absorber and the thermal-capture spectrum obtained with the target enriched in  $^{145}\text{Nd}$  where no boron absorber is used gives still better resolution (4.2 keV). There is no sign of a doublet structure at 6521.3 keV in any of these three spectra. The intensity of this line is reduced by a factor of 2 upon changing the boron absorber thickness from 0.32 to 0.95 cm. We conclude that unusually large Porter-Thomas fluctuations of  $\gamma$ -transition widths associated with the low-energy neutron resonances is the cause of the unusually large intensity of this line rather than doublet line structure. In addition, we have examined all possible low-energy lines which might connect with such a level and find that there are no doublet candidates. Our conclusion is that the existence of a  $2^+$  state very near (within 2 keV) to the 1043.1-keV state is unlikely.

A  $0^+$  state at 999.1 keV was suggested by Berzin *et al.*<sup>10</sup> based on  $\gamma$  transitions (from conversion electron data) to the  $0^+$  ground state and first  $2^+$  state. In our case the existence of a weak unplaced 545.4-keV  $\gamma$  ray ( $0^+ \rightarrow 2^+$ ) and the absence of a 999-keV  $\gamma$  ray ( $0^+ \rightarrow 0^+$ ) is consistent with their suggestion as is the fact that the  $(\bar{n}, \gamma)$  process produces no primary transition to the proposed  $0^+$  state. Berzin *et al.* place the 474.5-keV  $\gamma$  ray depopulating the 1470.8-keV level to this proposed level. The multiplet around the 474.5-keV  $\gamma$  ray contains a 471.4-keV  $\gamma$  ray which provides a more likely choice. We feel that more precision on the energies and intensities of members of this multiplet is needed before we place this  $\gamma$  ray (471.4 keV).

The placement of the 474.5-keV (7.5%) line causes intensity balance difficulties in several places where it could be fitted on an energy basis and its assignment at the 1470.8-keV level as suggested by Berzin *et al.*<sup>10</sup> would produce bad energy fits as well as the smallest input-to-output intensity ratio of any of the positive-parity excited states. We have made attempts to extend the level scheme an additional 1 MeV upwards and found that a great many of the unplaced  $\gamma$  rays could be fitted into the scheme. The input-to-output intensity ratio at the 1745.4-keV state can be increased from the 0.13 value for the present level scheme into the range of 0.45 to 0.85. However, this effort did not seem to help the 1470.8-keV case. We conclude that any extension of the level

scheme (Fig. 5) would best wait until we have measurements based on average neutron capture in a target enriched in  $^{145}\text{Nd}$ . The state proposed by Daniels *et al.*<sup>1</sup> and Berzin *et al.*<sup>10</sup> at 1224 keV cannot have  $J^\pi = 2^+, 3^+, 4^+, \text{ or } 5^+$  since there is no  $E1$  primary of the proper energy following average capture. We agree with the  $2^+$  assignment at 1473 keV made by Berzin *et al.*<sup>10</sup> Additional strong evidence for a  $2^+$  assignment for the first excited state comes from the heavy-ion ( $^{16}\text{O}$ ) Coulomb-excitation work reported by Eccleshall, Yates, and Simpson.<sup>23</sup>

#### Levels at 1745.4, 1777.7, and 1787.8 keV

As seen in Fig. 5, the next three levels at 1745.4, 1777.7, and 1787.8 keV are all positive-parity states. The first of these is a new state fed by a stronger  $E1$  primary suggesting that its spin is either 3 or 4. A level reported by Oakey *et al.*<sup>6</sup> [based on the  $^{149}\text{Sm}(n, \alpha)^{146}\text{Nd}$  reaction] may be the same state. Three possible transitions to the first three excited states are consistent with a  $J^\pi$  assignment of either  $3^+$  or  $4^+$  but as mentioned before the very low ratio of input-to-output intensity suggests that we have not extended the level scheme high enough in energy to locate very much of the input intensity. The level at 1777.7 keV was reported as a positive-parity state by Berzin *et al.*<sup>10</sup> and possibly by Reddingius<sup>12</sup> who tentatively suggested a state at 1780 keV. Due to the stronger  $E1$  primary  $\gamma$  transition to this state we know that its parity is positive and the spin is more likely to be either 3 or 4. Though we show only one transition depopulating this state to the  $2^+$  first excited state the  $\gamma$ -ray candidates for transitions to the first  $4^+$  and first  $3^+$  states may exist since they are each within 2 keV of very strong transitions of 735.9 and 589.4 keV, respectively (see Table V). As in the case of the first  $4^+$  state, the primary  $\gamma$  ray to this state was abnormally intense in the thinner-boron absorber spectrum but greatly reduced in the thick-absorber spectrum. Therefore, a spin of 2 is not ruled out. There is a possible weak ground-state transition (1777.3 keV) though we have placed it elsewhere in the level scheme. The third state of this group is also a new state with energy 1787.8 keV and  $J^\pi = 2^+$ . Four possible transitions going to the ground state and first three excited states allow us to make the spin assignment of 2 from among the two possibilities (2 or 5) suggested by the primary-transition intensity to this level.

#### Levels between 1800 and 2000 keV

With the possible exceptions of the 1884.7-, 1978.4-, 2357.0-, and 2516.3-keV states all the

remaining states are newly reported in this level scheme (Fig. 5). There are 24 states above 1800 keV, six of which have negative parity.

The levels at 1812.1 and 1884.7 keV appear to be fed by weak primary transitions from the capture state (see Fig. 4) and should therefore be negative-parity states. The isotopic identifications for these two transitions are uncertain. In addition, there appear to be no low-energy  $\gamma$  connections to these levels that are consistent with selection rules, so the evidence for the existence of these levels is weak. Therefore, they are dashed in the level scheme. If they do exist, the intensity errors do not allow us to distinguish between the two possible spin groups in either case, but the group composed of  $J=2$  or 5 seems favored.

The  $2^+$  level at 1919.1 keV is suggested by the  $E1$  primary transition and four transitions depopulating it to low-lying states. Various authors<sup>1,10,12</sup> have reported a state at about 3 keV below this energy but with no spin or parity assignments. The  $(n, \alpha)$  work by Oakey *et al.*<sup>6</sup> suggested a state at 1913 keV and Groshev *et al.*<sup>9</sup> reported a state at 1922 keV based on neutron-capture  $\gamma$  rays. Since the transitions go to the first and second  $2^+$  states and also the first  $4^+$  and  $3^-$  states, the spin choice of 5 allowed by the  $E1$  primary transition is ruled out in favor of the spin of 2.

The next level at 1978.4 keV is given a  $2^+$  assignment but the primary transition to this state falls between the two major intensity groupings and is the only case that does so (see Fig. 4). This line falls into the  $2^+$ ,  $5^+$  intensity group in the case of the spectrum obtained using the thinner (0.32-cm) boron absorber even though in general the averaging of intensities in this data was not as good as it was for the spectrum obtained using the thicker (0.95-cm) absorber. This state is reported by Daniels *et al.*<sup>1</sup> with three strong transitions depopulating the level. They conclude that  $J=2$  is most likely but they fail to determine the parity or to rule out  $J=3$ . We observe the same three transitions and a possible ground-state transition (1977.7 keV, 0.23). In our data the 602.0 keV is not only the weakest transition of the three (as in the case of the work by Daniels *et al.*<sup>1</sup>) but it is a member of a weak multiplet in the high-energy wing of the very strong 489.4-keV (27.0%) line (see Table V). Our measurements of this line for both energy and intensity are poor and the intensity is just barely above the threshold of sensitivity. The ground-state-transition energy and intensity errors are large since the line is unfolded from a multiplet. The 788.8-keV transition to the 1189.6-keV,  $3^-$  state establishes the energy of 1978.4 keV.

The 1989.5-keV state is assigned positive parity due to the weaker  $E1$  primary intensity and the spin-5 choice is ruled out by the three transitions shown depopulating the state. Groshev *et al.*<sup>9</sup> report a state at 1988 keV with no  $J^\pi$  assignments.

#### Levels above 2000 keV

Except for the  $2^+$  state at 2220.1 keV, the secondary transitions connected with the levels above 2000 keV do not give sufficient additional information to that contained in the primary transitions to allow final-spin choices to be made. Two of the 20 levels above 2000 keV have been reported by both Berzin *et al.*<sup>10</sup> and by Reddingius<sup>12</sup> without  $J^\pi$  assignments. One of these is the positive-parity state at 2357.0 keV and the other the negative-parity state at 2516.3 keV. One other level (2521.8 keV) was observed by Groshev *et al.*<sup>9</sup>

We have chosen to limit the level scheme at 2528.3 keV for a number of reasons. First, the complexity of the average-neutron-capture primary  $\gamma$ -ray spectrum for lower-energy primary transitions is sharply increased due to the primary transitions following capture in  $^{142}\text{Nd}$  and in  $^{144}\text{Nd}$ . Secondly, the level density in  $^{144}\text{Nd}$  and  $^{146}\text{Nd}$  has increased considerably. Thirdly, the signal-to-noise ratio of all lines of interest of any given neodymium isotope is considerably lower for the natural target than in a comparable size target which is enriched. This is because the natural target requires more material to get the same counting rate above background in a given line as that obtained with an enriched target, and that counting rate appears on the background created from all isotopes and concomitant contaminants.

We do have some reasonably good preliminary evidence for eight additional levels above the 2528.3-keV level and we have summarized this evidence in Table VII. The two primary  $\gamma$  transitions listed in parentheses have some uncertainty as to their isotopic origin since we did not observe them in the thermal runs; however, we believe their assignment to  $^{146}\text{Nd}$  is the most likely choice. Several of the transitions would create intensity imbalance for the final state involved if all the listed intensity were located as shown. Many lower-energy strong transitions are evident in the data down to at least 4 MeV and some of these are sure to be primary transitions in  $^{146}\text{Nd}$  to positive-parity states.

#### Rotational sequences

We have examined the levels shown in Fig. 5 plus those listed in Table VII for possible rotational bands. There are some reasonable candi-

TABLE VII. Possible levels above 2600 keV suggested by average-resonance neutron-capture and low-energy transitions. Due to the increasing complexity of the spectrum which came from natural-abundance targets, some of these levels are deemed too speculative to include in the level scheme. Others create intensity-balance problems for the final states to which transitions appear to occur. The level energy in column 2 is given by  $E_L = E_0 - E_\gamma$  where  $E_0 = 7564.7$  keV. The values of  $J^\pi$  predicted by the average-capture data ( $\bar{n}, \gamma$ ) are given in column 3.

Primary $E_\gamma$ (keV)	$E_L$ (keV)	$J^\pi$ via ( $\bar{n}, \gamma$ )	Secondary $E\gamma(I\gamma)$ (keV)	$E_L$ (keV)	Final State $J^\pi$
(5016.9)	2547.8	$2^+, 5^+$	1502.9 (0.22)	1043.1	$4^+$
			1169.5 (0.30)	1377.1	$1^-$
5011.9	2552.8	$2^+, 5^+$	1363.5 (0.79)	1189.6	$3^-$
			807.3 (0.70)	1745.4	$3^-, 4^+$
			765.1 (0.12)	1787.8	$2^+$
			479.2 (0.83)	2073.2 <sup>a</sup>	$3^-, 4^-(2^-, 5^-)$
(5008.7)	2556.0	$3^+, 4^+$	578.0 (0.29)	1978.4	$2^+$
			565.1 (0.25)	1989.5	$2^+$
5002.5	2562.2	$2^+, 5^+$	2108.3 (0.46)	453.7	$2^+$
			677.1 (0.10)	1884.7	$2^-, 5^-(3^-, 4^-)$
4990.9	2573.7	$3^+, 4^+$	2120.2 (0.38)	453.7	$2^+$
			584.6 (0.32)	1989.5	$2^+$
4975.1	2589.6	$3^+, 4^+$	2136.0 (0.71)	453.7	$2^+$
			600.0 (0.12)	1989.5	$2^+$
4963.1	2601.6	$3^-, 4^-(2^-, 5^-)$	528.3 (0.45)	2073.2 <sup>a</sup>	$3^-, 4^-(2^-, 5^-)$
4903.8	2660.9	$3^+, 4^+$	2207.0 (0.23)	453.7	$2^+$
			[1471.0 (4.4)] <sup>b</sup>	1189.6	$3^-$
			1190.8 (0.30)	1470.8	$2^+$
			883.3 (1.1)	1777.7	$3^+, 4^+$
			565.1 (0.25)	2096.3	$2^+, 5^+(3^+, 4^+)$

<sup>a</sup> Transition into the final state is too strong compared to the intensity depopulating the state.

<sup>b</sup> A part of the line intensity could be located here but most of it is believed to be in the  $\gamma$  line connecting the 1470.8-keV level and the ground state.

dates based on energy spacings alone but the corresponding intraband transition energies generally fall below the range of the low-energy spectrum obtained in this work. One possible band based on an octupole vibration is: 1377.1 keV ( $1^-$ ), 1812.0 keV ( $3^-$ ), and 2601.6 keV ( $5^-$ ). Another possibility based on a  $\gamma$  vibration is: 1470.8 keV ( $2^+$ ), 1777.7 keV ( $3^+$ ), 2197.3 keV ( $4^+$ ), and 2707 keV ( $5^+$ ). The members of both of these band possibilities fall very close to a straight line when  $E_L$  (level energy) is plotted vs  $J(J+1)$ .

There are additional possible primary transitions to positive-parity states (up to 3230 keV) indicated in both the average-capture spectra (one using 0.32 cm of boron and one with 0.96 cm of boron) whose isotopic identities are too uncertain to include in the level scheme. We have used 11 of these to extend the level scheme and search for other band possibilities. There are at least eight additional bands whose members conform to a rotational-energy spacing sequence.

To extend the level scheme to higher energies we are planning to obtain average-resonance

neutron-capture  $\gamma$ -ray spectra from a target highly enriched in  $^{145}\text{Nd}$ .

## DISCUSSION

Since the  $^{146}\text{Nd}$  nucleus has 86 neutrons, it has 4 neutrons beyond the spherical closed shell, and is somewhat deformed so that the characteristic pattern for a vibrational nucleus is not so completely maintained. Even the two-phonon triplet is not established in this case since only a possible member at 1043.1 keV has been described in the region of the two-phonon energy. If one assumes that the  $2^+$  member of the predicted two-phonon triplet is not near the  $4^+$  member as discussed earlier, then all the  $2^+$  states are observed and the nearest candidate for the  $2^+$  member is far enough away (at 1470.8 keV) that a simple vibrational model may not be appropriate. The data discussed in this paper were also used to identify many lines in the  $^{143}\text{Nd}(n, \gamma)^{144}\text{Nd}$  spectrum and to construct a preliminary level scheme for  $^{144}\text{Nd}$ . This nucleus has only two neutrons beyond



the closed shell at  $N=82$  and therefore might be even a better vibrator, but again the nearest  $2^+$  candidate (at 1560.8 keV) for the  $2^+$  member of the two-phonon triplet is rather far from the  $4^+$  member at 1313.9 keV. The absence of the  $2^+$  member occurs in many nuclei on the other side of the closed neutron shell at  $N=82$  as well, for example, Te isotopes.<sup>24</sup> One of the newer phonon

models such as the interacting boson model described by Iachello and Arima<sup>25</sup> may be more appropriate for the Nd nuclei.

Quasirootational bands built on both  $\beta$  and  $\gamma$  vibrations are suggested for  $^{146}\text{Nd}$  based on energy spacing, but additional low-energy spectroscopy is needed to establish intraband transitions.

\*Work supported by the U. S. Energy Research and Development Administration.

<sup>1</sup>W. R. Daniels, F. O. Lawrence, and D. C. Hoffman, Nucl. Phys. **A118**, 467 (1968).

<sup>2</sup>A. V. Ramayya and Y. Yoshizawa, Phys. Rev. **137**, B13 (1965).

<sup>3</sup>D. J. Buss, E. G. Funk, and J. W. Mihelich, Phys. Rev. **141**, 1193 (1966).

<sup>4</sup>H. W. Taylor and A. H. Kukoc, Nucl. Phys. **A122**, 425 (1968).

<sup>5</sup>M. P. Avontina, E. P. Grigor'ev, A. V. Zolotavin, V. O. Sergeev, M. I. Sovtsov, M. Weiss, J. Urbanec, J. Vrzal, and J. Liptak, Yad. Fiz. **11**, 1133 (1970) [Sov. J. Nucl. Phys. **11**, 629 (1970)].

<sup>6</sup>N. S. Oakey and R. D. McFarlane, Phys. Lett. **24B**, 142 (1967).

<sup>7</sup>F. Poortmans, H. Ceulemans, A. J. Deruytter, and M. Neve De Mavergnies, Nucl. Phys. **82**, 331 (1966).

<sup>8</sup>P. T. Christensen, G. Lóvhóiden, and J. Rasmussen, Nucl. Phys. **A149**, 302 (1970).

<sup>9</sup>L. V. Groshev, V. N. Dvoret'skii, A. M. Demidov, and A. S. Rakhimov, Yad. Fiz. **8**, 1967 (1968) [Sov. J. Nucl. Phys. **8**, 619 (1969)].

<sup>10</sup>Ya. Ya. Berzin, A. E. Kruminya, and P. T. Prokof'ev, Izv. Akad. Nauk SSSR, Ser. Fiz. **34**, 824 (1970) [Bull. Acad. Sci. USSR, Phys. Ser. **34**, 733 (1970)].

<sup>11</sup>E. R. Reddingius, J. F. M. Potters, and H. Postma, Physica **38**, 48 (1968).

<sup>12</sup>E. R. Reddingius, Ph.D. thesis, 1969 (unpublished).

<sup>13</sup>L. M. Bollinger and G. E. Thomas, Phys. Rev. C **2**, 1951 (1970).

<sup>14</sup>Resonance Parameters, S. F. Mughabghab and D. J. Garber, Brookhaven National Laboratory Report No. BNL-325 (National Technical Information Service, Springfield, Va., 1973), 3rd. ed., Vol. I, p. c/169.

<sup>15</sup>G. E. Thomas, D. E. Blatchley, and L. M. Bollinger,

Nucl. Instrum. Methods **56**, 325 (1967).

<sup>16</sup>R. C. Greenwood, Phys. Lett. **27B**, 274 (1968).

<sup>17</sup>G. E. Thomas, Argonne National Laboratory (private communication).

<sup>18</sup>M. G. Strauss, F. R. Lenkszus, and J. J. Eickholz, Nucl. Instrum. Methods **76**, 285 (1969); ANL Report No. ANL-7282, 1966 (unpublished), p. 113.

<sup>19</sup>J. K. Hawkins, Master's thesis, Northern Illinois University, 1974 (unpublished).

<sup>20</sup>D. L. Hillis, C. R. Bingham, D. A. McClure, N. S. Kendrick, Jr., J. C. Hill, S. Raman, J. B. Ball, and J. A. Harvey, Phys. Rev. C **12**, 260 (1975).

<sup>21</sup>N. R. Najam, A. F. M. Ishaq, M. Anwar-ul-Islam, A. M. Khan, and A. J. Mirza, in *Proceedings of the Second International Symposium on Neutron Capture  $\gamma$ -Ray Spectroscopy and Related Topics, Petten, 1974* (Reactor Centrum Nederland, Petten, 1975), p. 365.

<sup>22</sup>J. A. Mirza, A. M. Khan, M. Irshad, H. A. Schmidt, A. F. M. Ishaq, and M. Anwar-ul-Islam, in *Proceedings of the Second International Symposium on Neutron Capture  $\gamma$ -Ray Spectroscopy and Related Topics* (see Ref. 21), p. 357.

<sup>23</sup>D. Eccleshall, M. J. L. Yates, and J. J. Simpson, Nucl. Phys. **78**, 481 (1966).

<sup>24</sup>D. L. Bushnell, R. P. Chaturvedi, and R. K. Smither, Phys. Rev. **179**, 1113 (1969).

<sup>25</sup>F. Iachello, in *Proceedings of the International Conference on Nuclear Structure and Spectroscopy, Amsterdam, 1974*, edited by H. P. Blok and A. E. L. Dieparink (Scholar's Press, Amsterdam, 1974), Vol. 2, p. 163; F. Iachello and A. Arima, in *Proceedings of the Topical Conference on Problems of Vibrational Nuclei, Zagreb, Yugoslavia, September, 1974*, edited by G. Alaga, V. Paar, and L. Sips (North-Holland, Amsterdam, 1974).